

NON-UNIFORM WATER FLUX DENSITY APPROACH APPLIED ON A MATHEMATICAL MODEL OF HEAT TRANSFER AND SOLIDIFICATION FOR A CONTINUOUS CASTING OF ROUND BILLETS

Charles Assunção¹
Roberto Parreiras Tavares²
Guilherme Oliveira³

Abstract

In the present work, the water flux densities of nozzles with flat jet and full cone jet were experimentally measured using an apparatus in industrial scale that reproduces the secondary cooling of the continuous casting of round billets of Vallourec Tubos do Brasil. A mathematical model for heat transfer and solidification for the continuous casting of round billets was developed applying the experimental water flux density profile, establishing a non-uniform water distribution approach. The mathematical model was validated by experimental measurements of the billet superficial temperature, performed at the industrial plant. The results of the mathematical model using both uniform and non-uniform water flux density approaches were compared. The non-uniform water distribution approach enabled to identify important variations of the heat transfer coefficients and the billet temperatures, especially in the first cooling zone, and to assess more accurately the local effects of the water distribution on the thermal behavior of the strand. The non-uniform water flux density approach applied to the mathematical model was a useful and more accurate tool to improve the comprehension of the thermal behavior of the steel along the secondary cooling.

Keywords: Water flux density; Heat transfer coefficient; Secondary cooling; Mathematical model.

DISTRIBUIÇÃO NÃO-UNIFORME DA VAZÃO ESPECÍFICA DE ÁGUA APLICADA AO MODELO MATEMÁTICO DE TRANSFERÊNCIA DE CALOR E SOLIDIFICAÇÃO DO LINGOTAMENTO CONTÍNUO DE BARRAS CILÍNDRICAS

Resumo

As vazões específicas de água de bicos spray com jato do tipo leque e cone cheio foram medidas experimentalmente usando um aparato em escala industrial que reproduz o resfriamento secundário do lingotamento contínuo de barras cilíndricas da Vallourec Tubos do Brasil. Um modelo matemático da transferência de calor e solidificação foi desenvolvido aplicando o perfil de vazão específica de água obtida experimentalmente, desenvolvendo uma nova abordagem de distribuição não-uniforme de água. O modelo matemático foi validado por medições experimentais de temperatura superficial da barra realizadas na planta industrial. Os resultados do modelo matemático usando as abordagens de distribuição uniforme e não-uniforme de vazão específica de água foram comparados. A abordagem de distribuição não-uniforme de vazão específica de água permitiu identificar importantes variações no coeficiente de transferência de calor e na temperatura superficial da barra, especialmente na primeira zona de resfriamento por spray, e, conseqüentemente, avaliar de forma mais exata os efeitos localizados na distribuição de água no comportamento térmico do aço. A abordagem de distribuição não-uniforme de vazão específica de água se mostrou uma ferramenta útil e mais acurada para aumentar a compreensão do comportamento térmico do aço ao longo da câmara spray.

Palavras-chave: Vazão específica de água; Coeficiente de transferência de calor; Resfriamento secundário; Modelo matemático.

¹Mechanical Engineer, Dr., Vallourec Tubos do Brasil, Belo Horizonte, MG, Brazil. E-mail: charles.assuncao@vallourec.com

²Metalurgist Engineer, PhD, Universidade Federal de Minas Gerais – UFMG, Belo Horizonte, MG, Brazil. E-mail: rtavares@demet.ufmg.com

³Metalurgist Engineer, Undergraduate student, Universidade Federal de Minas Gerais – UFMG, Belo Horizonte, MG, Brazil. E-mail: guilhermedias@ufmg.br

1 INTRODUCTION

The continuous growing demand of steel and the development of new applications increase the competitiveness and make the quality of the products one of the most important factors for the survival of the steel manufacturers. The quality of the steel in the continuous casting is directly related to the temperature variation during the solidification process [1]. Inappropriate temperature profiles can cause defects such as cracks, deep oscillation marks, depressions, inclusions and geometric deviation [2]. The knowledge of the thermal behavior of the steel is mandatory to define the best operational practices and, consequently, to reduce quality issues. Probably, the most common method to analyze the heat transfer phenomena during the continuous casting of steel is the mathematical modeling. The first mathematical models of heat transfer and solidification of steel in the continuous casting were developed by Mizikar [3] and Lait et al. [4]. Since then, several other mathematical models have been developed. In the mold, the superficial heat flux of the steel can be calculated relating the residence time inside the mold and the average heat flux [5-10]. An alternative approach that has been largely applied [11-14] is to use the inverse problem of heat conduction through the mold wall. In the secondary cooling zone, the superficial heat flux of steel involves different mechanisms, such as radiation in the dry zones, conduction in the roll contacts and convection due to the water sprays [15]. The heat extraction in the spray zone depends on the water pressure, stand-off distance between the strand and the nozzle, nozzle type, strand surface temperature and water flux. Exhaustive studies have been developed to identify the effect of these parameters of spray on the heat flux [16,17]. Most of these studies have been performed in laboratory where a hot steel plate is cooled using commercial nozzles. All the studies agree that, in the temperature range of interest, the water flux has the largest effect on the heat transfer coefficient. Some authors have measured the water flux density of different types of nozzles [18,19] for slabs and square billets and the common conclusion is that the water flux distribution is not uniform. Since the water flux density varies locally along the secondary cooling zone, the heat flux and heat transfer coefficient vary locally as well. However, the results of the non-uniformity of water distribution have not been largely used in the heat transfer modeling [20-22]. This assumption can lead to imprecision, especially in the evaluation of local phenomena. Besides that, no reference of water flux density for round billets has been found in literature. Therefore, the objectives of the present work are to determine experimentally the water flux density of flat jet and full cone jet nozzles along the secondary cooling zone, to develop a mathematical model of heat transfer and solidification of steel and to investigate the effect of the non-uniformity of the water distribution on heat transfer coefficients and billet temperatures.

2 METHODOLOGY

2.1 Mathematical Model

The mathematical model of heat transfer and solidification of the billet has been developed for a continuous casting machine of round billets. This machine has four strands and is capable of producing billets of 180 mm and 230 mm diameters. The mathematical model takes into account the heat transfer by conduction in both radial and angular direction. The main assumptions are listed below:

- Symmetry of transversal section, only one eighth of the transversal section was modeled, as shown in Figure 1;
- The heat transfer by conduction in the casting direction was neglected due to the high Peclet number;
- The latent heat of solidification was converted into an equivalent specific heat capacity in the mushy zone;
- The density of the steel was considered constant whereas the heat capacity, thermal conductivity and emissivity were temperature-dependent;
- The effects of strand shrinkage were neglected;
- The convective heat flow in the liquid pool and mushy zone was accounted for the effective thermal conductivity [9].

The strand was divided into several slices of steel that move downwards in the casting direction at the casting speed. The domain of the model was divided in 400 control volumes with 40 divisions in the radial direction and 10 divisions in the angular direction. The energy balance was applied on each control volume in a time interval of calculation (Δt) equal to 0.01 s.

The energy balance was obtained from the general energy conservation equation for cylindrical coordinates. In order to obtain the numerical solution, the Equation 1 was discretized and explicitly solved by the finite volume method [23].

$$\rho \frac{\partial (C_p^{eq} T)}{\partial t} = \frac{1}{r} \frac{\partial}{\partial r} \left(r k_{ef} \frac{\partial T}{\partial r} \right) + S \quad (1)$$

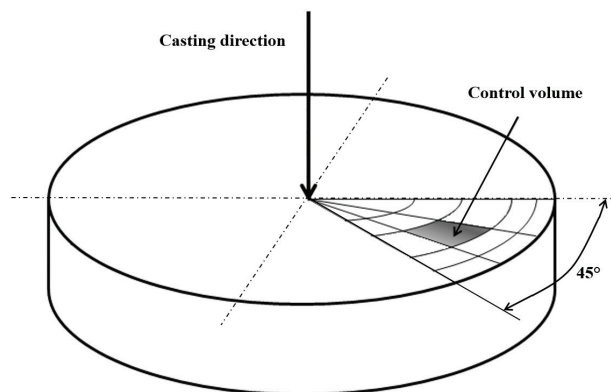


Figure 1. Mathematical model domain.

where ρ is the density of steel [$\text{kg}\cdot\text{m}^{-3}$]; C_p^{eq} is the equivalent heat capacity of steel [$\text{J}\cdot\text{kg}^{-1}\cdot\text{K}^{-1}$]; r is the radial position of the control volume [m]; k_{ef} is the effective thermal conductivity of steel [$\text{W}\cdot\text{m}^{-1}\cdot\text{K}^{-1}$]; T is the temperature of steel [K]; t is time [s]; S is the source term used to consider the boundary conditions [$\text{W}\cdot\text{m}^{-3}$].

The solidification was considered under equilibrium conditions and the liquid fraction of the steel was determined by means of the lever rule Equations 2 and 3 [24].

$$f_{\text{liq}} = \frac{(T_0 - T_L) - k(T_0 - T)}{(1-k)(T_0 - T)} \quad (2)$$

$$k = \frac{T_0 - T_L}{T_0 - T_S} \quad (3)$$

where T_0 is the melting temperature of pure iron [K], T_L is the liquidus temperature of the steel [K], T is the temperature of steel [K] and k is the partition coefficient.

The equivalent heat capacity of steel in mushy zone was calculated considering the effect of latent heat of steel solidification (Equations 4 and 5).

$$C_p^{\text{eq}} = C_p + L \frac{df_{\text{liq}}}{dT} \quad (4)$$

$$\frac{df_{\text{liq}}}{dT} = \frac{(T_0 - T_L)}{(1-k)(T_0 - T)^2} \quad (5)$$

where C_p is heat capacity of solid steel [$\text{J}\cdot\text{kg}^{-1}\cdot\text{K}^{-1}$] and L is the latent heat of steel solidification [$\text{J}\cdot\text{kg}^{-1}$];

The convective effects in the liquid portion of steel were considered using an effective thermal conductivity (Equation 6).

$$k_{\text{ef}} = k_{\text{sol}} \left[1 + (C-1)f_i^2 \right] \quad (6)$$

where f_i is the liquid fraction of steel in the mushy zone, C is a constant equal to 6 and K_{sol} is the thermal conductivity of the solid steel.

In order to validate the model, the superficial temperature of the billet was measured by two-color pyrometers at the exit of each cooling zone in the spray chamber, i.e., at the distances from the meniscus $z=1.30\text{m}$, $z=4.07\text{m}$, $z=7.65\text{m}$ and $z=11.5\text{m}$.

2.1.1 Boundary conditions

The initial condition is $T_{\text{steel}} = T_{\text{tundish}}$, i.e., the temperature of steel is the same as that measured in the tundish.

In the mold, the boundary condition was expressed in terms of an average heat flux [5] [$\text{MW}\cdot\text{m}^{-2}$], as shown by Equation 7.

$$q_{\text{mold}} = \alpha(2,679 - 0,221\sqrt{t_{\text{mold}}}) \quad (7)$$

where t_{mold} is the residence time of each slice of steel inside de mold and α [dimensionless] is the calibration factor for each cooling zone.

In the secondary cooling, the heat flux [$\text{W}\cdot\text{m}^{-2}$] was calculated by the Equations 8, 9 and 10 [19].

$$q_{\text{spray}} = h_g (T_{\text{steel}} - T_{\text{water}}) \quad (8)$$

$$h_{\text{conv}} = \alpha(708W^{0,75}T_{\text{steel}}^{-1,2} + 0,116) \quad (9)$$

$$h_{\text{conv}} = \alpha(708W^{0,75}T_{\text{steel}}^{-1,2} + 0,116) \quad (10)$$

where h_g is the global heat transfer coefficient [$\text{W}\cdot\text{m}^{-2}\cdot\text{K}^{-1}$], T_{steel} is the superficial temperature of steel [K], T_{water} is the temperature of the water spray [K], h_{conv} is the convection heat transfer coefficient [$\text{W}\cdot\text{m}^{-2}\cdot\text{K}^{-1}$], T_{∞} is the environment temperature [K] and W is the water flux density [$\text{l}\cdot\text{s}^{-1}\cdot\text{m}^{-2}$].

The calibration factors α were used to adjust the equations of the mold heat flux and the convection heat transfer coefficient obtained in the literature references [5,19] to the plant data. In the mold, α relates the heat transfer calculated by Equation 7 and the heat transfer calculated using the temperature variation and the flow rate of the cooling water. In the secondary cooling zone, α was obtained through the strand superficial temperature measurements. The factor α was varied in order to adjust the model results with the experimental results of temperature in all range of casting speed.

2.1.2 Physical properties of the steel

The physical properties of steel considered in the model are shown in Table 1.

2.2 Experimental Procedures

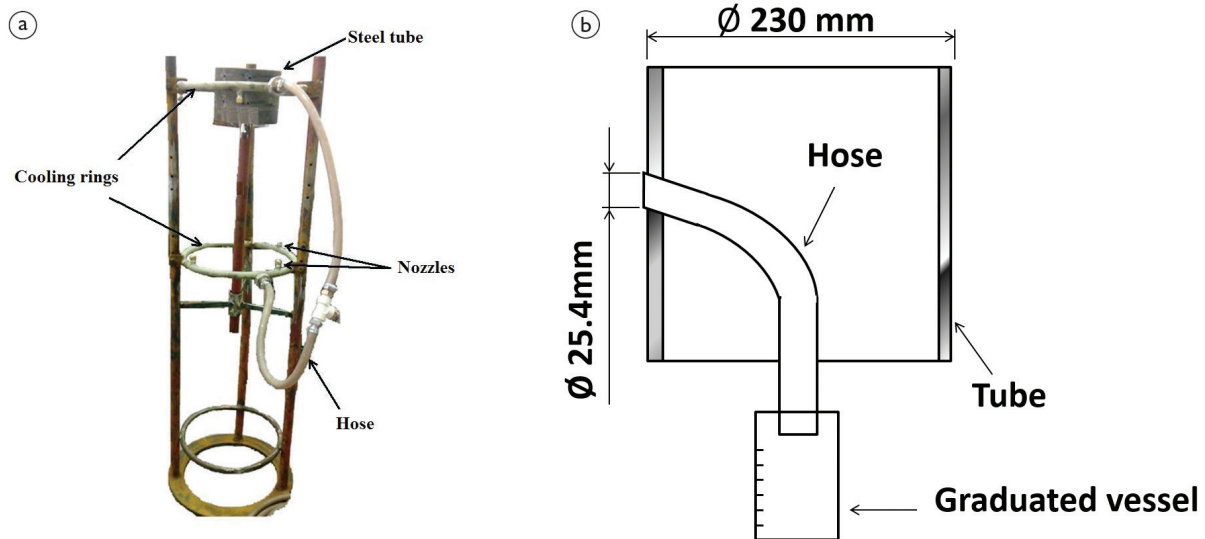
The experimental procedures described in this section were performed to obtain the water flux density distribution at several positions along the secondary cooling zones.

Figure 2 shows the apparatus that was used. The apparatus had the same size and curvature of an actual strand. The spray rings were connected to a flexible hose connected to the system that supplied water to the nozzles. The nozzles used in the experiments were of the same type of those used in the actual plant. A small steel tube of outer diameter of 230 mm with a hole of 25.4 mm of diameter in the wall was positioned at several locations in the impingement area of the water spray. In order to collect the impinging water, a hose was connected to the hole and conducted the water to a graduated vessel.

In the experiments corresponding to zone 0, nozzles $1/4 \text{ U} - 5010$ (Spraying Systems) were used. This kind of nozzle has maximum flow rate of $10 \text{ l}\cdot\text{min}^{-1}$, a pulverization angle of 50° and a flat jet with a rectangular impingement area. For zones A, B and C, nozzles $1/4 \text{ GGA} - 3.9$ (Spraying

Table 1. Physical properties of steel

Parameter	Value
Density [25] [$\text{kg}\cdot\text{m}^{-3}$]	7020
Latent heat of solidification [25] [$\text{J}\cdot\text{kg}^{-1}$]	272000
Solidus temperature [26] [K]	$1809 - 415.5\%C + 12.3\%Si + 6.8\%Mn + 124.5\%P + 183.9\%S + 4.1\%Al$
Liquidus temperature [26] [K]	$1809 - 78\%C + 7.6\%Si + 4.9\%Mn + 34.4\%P + 38\%S + 3.6\%Al$
Specific heat [27] [$\text{J}\cdot\text{kg}^{-1}$]	$C_p = 481.482 + 0.1997\cdot T_{\text{steel}}$
Thermal conductivity [27] [$\text{W}\cdot\text{m}^{-1}\cdot\text{K}^{-1}$]	$k_{\text{sol}} = 15.9106 + 0.1151\cdot T_{\text{steel}}$
Emissivity [28]	$\varepsilon = 0.0002\cdot T_{\text{steel}} + 0.6274$

**Figure 2.** Experimental devices: (a) strand apparatus; (b) collecting water set.

Systems) were used. This nozzle has maximum water flow rate of $3,9 \text{ l}\cdot\text{min}^{-1}$, a pulverization angle of 79° and a full cone jet with a circular impingement area. Figure 3 shows the measurement positions.

3 RESULTS AND DISCUSSION

The results of water distribution measurements were applied on the mathematical model of heat transfer and solidification and the effects of the non-uniformity of water flux density were assessed. Figure 4 shows the water flux density along the cooling zones for a casting speed of $1.3 \text{ m}\cdot\text{min}^{-1}$ considering both the uniform water flux density [29], which is widely applied on the mathematical model, and the non-uniform water flux density, which considers the experimental results. Although the total amount of water is the same, the water distribution profiles generated by each approach are totally different. In zone 0, the uniform water flux density is $2.05 \text{ l}\cdot\text{s}^{-1}\cdot\text{m}^{-2}$, whereas the non-uniform water flux density has peaks greater than $50 \text{ l}\cdot\text{s}^{-1}\cdot\text{m}^{-2}$ in very

small areas at the cooling rings positions that produce a local overcooling. In zones A, B and C the differences between the water flux density calculated by each approach are smoother, but they can reach three times one from another.

The non-uniformity of water density has an important effect on the heat extraction of the billet, since the local water flux density is the main factor that affects the heat transfer by convection [17]. Figure 5 shows the profile of the global heat transfer coefficient in the longitudinal direction for angles 0° and 45° of the billet obtained by both water flux density approaches.

There are significant differences between the results of both uniform and non-uniform water flux density approaches along the entire strand. The non-uniform water flux density approach was capable to identify very intense and localized variations in the global heat transfer coefficient. At the positions where the water spray impinges in zone 0, the global heat transfer coefficient is greater than $6.0 \times 10^3 \text{ W}\cdot\text{m}^{-2}\cdot\text{K}^{-1}$, whereas at the dry areas, it is smaller than $2.2 \times 10^2 \text{ W}\cdot\text{m}^{-2}\cdot\text{K}^{-1}$, and this variation occurs in a longitudinal distance smaller than one centimeter. If the uniform

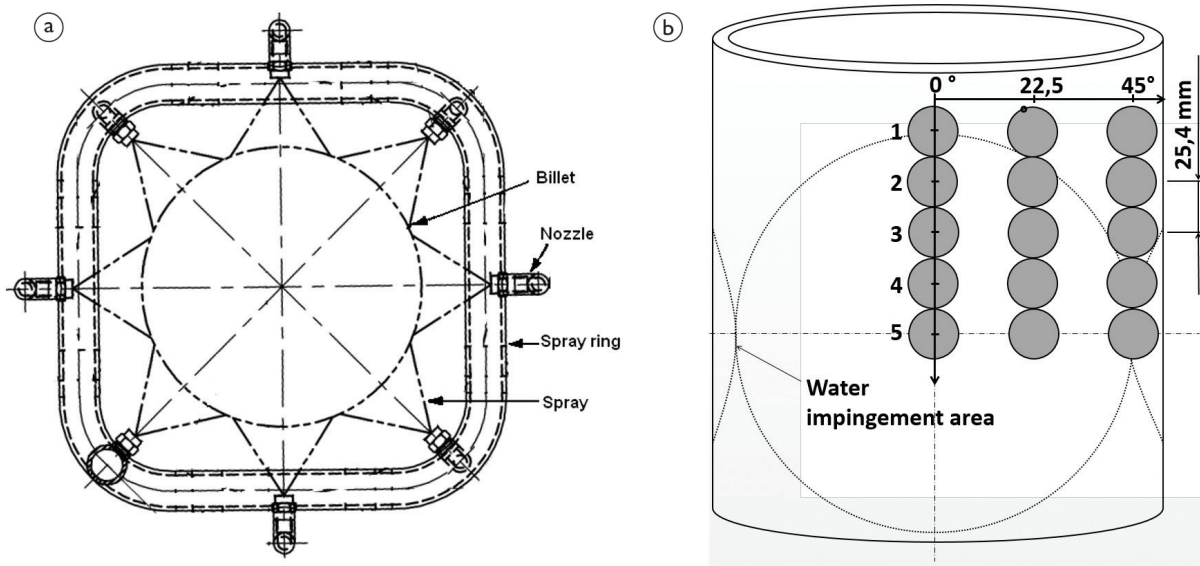


Figure 3. Positions of water distribution measurements: (a) angular positions for zone 0 ring; (b) angular and longitudinal positions for zones A, B and C.

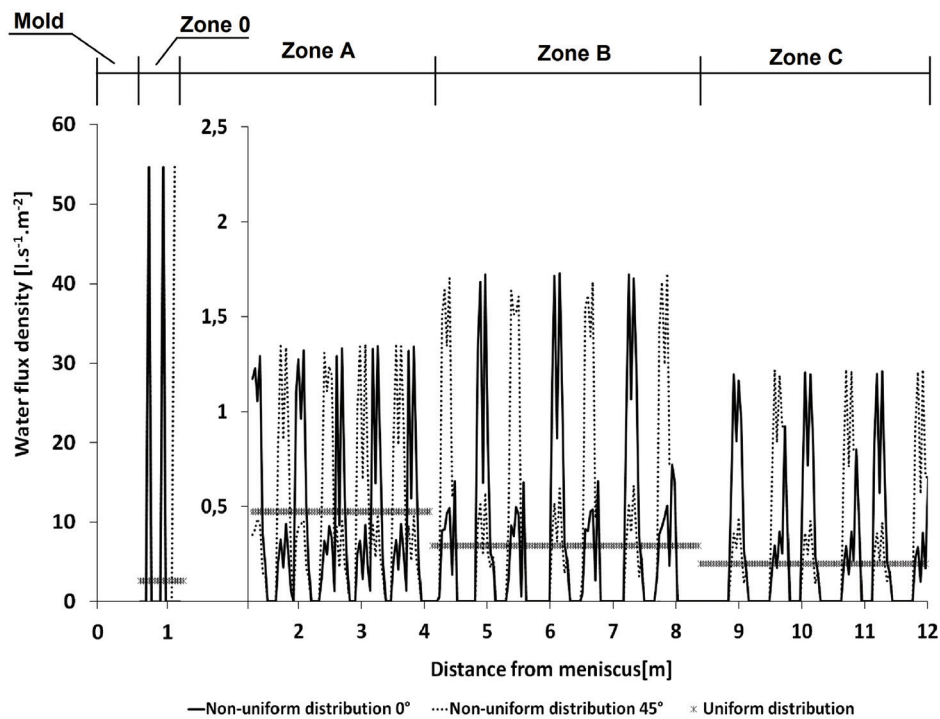


Figure 4. Water flux density along the strand.

water flux density was considered, the global heat transfer coefficient would be approximately $5.0 \times 10^2 \text{ W.m}^{-2}\text{K}^{-1}$ along the whole zone. In zones A, B C, the variations of the global heat transfer are smoother because the water flux density is less non-uniform than in zone 0, but it is possible to observe the differences between the results of both water distribution approaches in these zones as well.

From the global heat transfer coefficient profile, the superficial temperature of the strand was obtained,

as shown in Figure 6. The superficial temperature profile, calculated by the uniform water flux density, varies very smoothly along the secondary cooling zone. This result agrees with the results of other authors [30,31]. On the other hand, the non-uniform water flux density identifies zones of very intense temperature variation in both longitudinal and angular direction and gives a superficial temperature profile that oscillates inversely with the water flux density and the global heat transfer coefficient. At

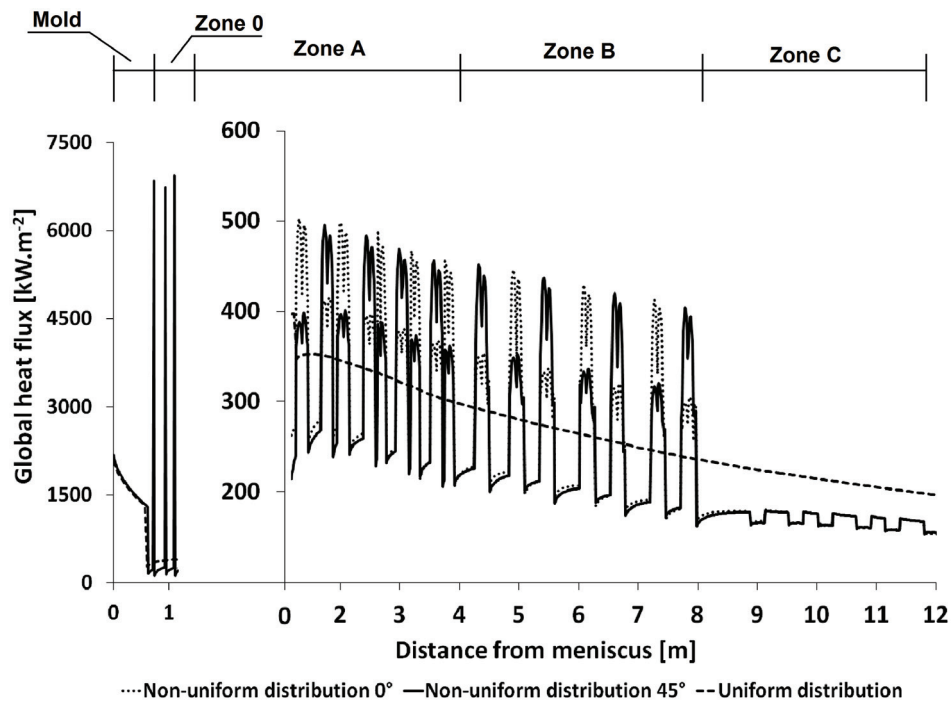


Figure 5. Global heat transfer coefficient along the strand.

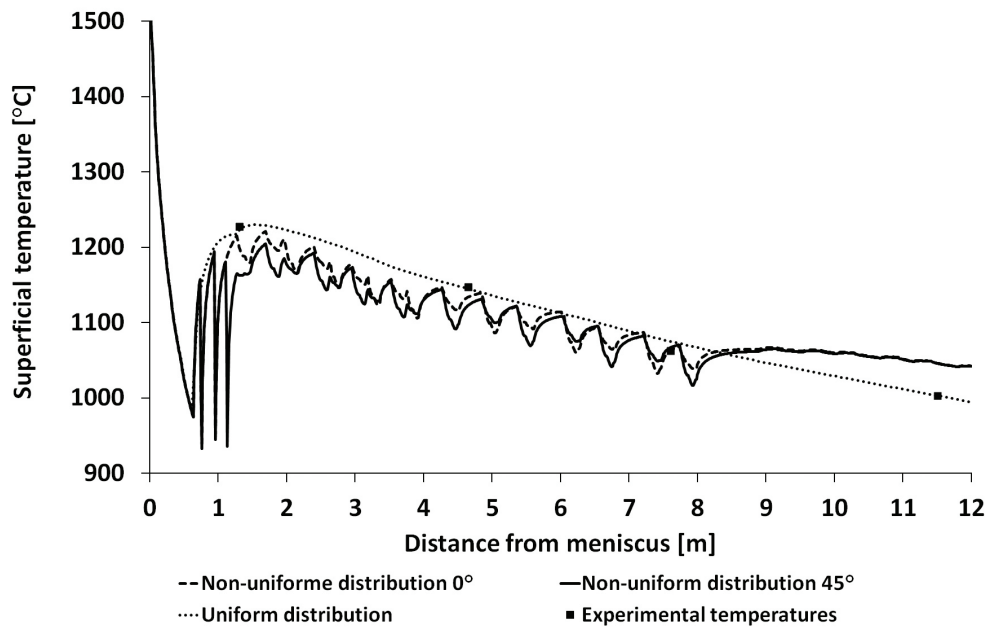


Figure 6. Superficial temperature along the strand.

the positions after the three spray rings, the temperature variations are larger than 230°C.

According to the results of the non-uniform water flux density, after leaving the mold, the slice of steel runs long enough distances to reheat and then it is submitted to a very high and concentrated cooling. The temperature variation of 230°C after the spray rings is much higher than the acceptable limit of 100°C [19]. These In zones A, B and C, the variation of the superficial temperature in the

longitudinal direction is smaller than in zone 0, however, it is possible to observe temperature variation of 50°C at some positions. These temperature variations could result in longitudinal internal cracks, midradial cracks, and longitudinal depressions with subsurface longitudinal facial cracks [18].

Several mathematical models of the heat transfer for the continuous casting machine have been developed. However, the non-uniformity of water flux density distribu-

tion in secondary cooling zone has been widely neglected, even though it is known that the water flux density provided by the conventional nozzles is not uniform. The consideration of uniform water flux density can lead to important errors in the thermal analysis of the strand, especially for local thermal phenomena. The non-uniform water flux density approach is capable to provide more realistic and detailed results, becoming a useful tool in the analysis and simulation of local thermal phenomena.

4 CONCLUSION

A mathematical model of the heat transfer and solidification for a continuous casting of round billet was developed and validated with superficial temperature measurements in an industrial plant. Experimental measurements of water flux density in the secondary cooling zone were performed using flat jet and full cone jet nozzles. The experimental results of the water flux density were inputted into the mathematical model through a water distribution coefficient, developing an innovative non-uniform water flux density approach. The results of this approach were compared with the results of the traditional uniform water

flux density approach. The most important difference found between both approaches is the capacity of this novel approach to characterize the local thermal phenomena of the strand. With the non-uniform water flux density, it was possible to identify important variations in the heat transfer coefficient and superficial temperature profiles in both longitudinal and angular directions. This non-uniform water distribution approach applied to the mathematical model has been found a useful and more accurate tool to enhance the comprehension about the thermal behavior of the steel along the secondary cooling in the continuous casting of round billets and to improve the analysis of the local thermal phenomena.

Acknowledgements

The financial support of FAPEMIG – Fundação de Amparo à Pesquisa do Estado de Minas Gerais, Brazil - in the form of a research grant to R. Tavares, Process No. TEC - APQ-00373-11, is gratefully acknowledged. The authors also acknowledge the financial support of CAPES to the graduate program.

REFERENCES

- 1 Sabau A. Measurement of heat flux at metal/mould interface during casting solidification. *International Journal of Cast Metals Research*. 2006;19(3):188-194. <http://dx.doi.org/10.1179/136404606225023390>.
- 2 Hebi Y, Man Y, Dacheng F. 3-D inverse problem continuous model for thermal behavior of mould process based on the temperature measurements in plant trial. *ISIJ International*. 2006;46(4):539-545. <http://dx.doi.org/10.2355/isijinternational.46.539>.
- 3 Thomas BG. Modeling of continuous casting of steel – past, present and future. *Metallurgical and Materials Transactions*. 2002;33(6):795-812. <http://dx.doi.org/10.1007/s11663-002-0063-9>.
- 4 Lait J, Brimacombe JK, Weinberg F. Mathematical modeling of heat flow in the continuous casting of steel. *Ironmaking & Steelmaking*. 1974;2:90-97.
- 5 Brimacombe JK. Design of continuous casting machines based o heat-flow analysis: state-of-the-art review. *Canadian Metallurgical Quarterly*. 1976;15:17-28.
- 6 Spuy D, Craig I, Pistorious P. An optimization procedure for the secondary cooling zone of a continuous billet caster. *Journal of the South African Institute of Mining and Metallurgy*. 1999;1:49-54.
- 7 Petrus B, Zheng K, Zhou X, Thomas BG, Bentsman J. Real-time, model-based spray-cooling control system for steel continuous casting. *Metallurgical and Materials Transactions*. 2011;42(1):87-103. <http://dx.doi.org/10.1007/s11663-010-9452-7>.
- 8 Choudhary S, Mazumdar D, Ghosh A. Mathematical Modelling of Heat Transfer Phenomena in continuous casting of steel. *ISIJ International*. 1993;33(7):764-774. <http://dx.doi.org/10.2355/isijinternational.33.764>.
- 9 Ma J, Xie Z, Jia G. Applying of real-time heat transfer and solidification model on the dynamic control system of billet continuous casting. *ISIJ International*. 2008;48(12):1722-1727. <http://dx.doi.org/10.2355/isijinternational.48.1722>.
- 10 Camisani-Calzolari FR, Craig IK, Pistorious PC. Specification framework for control of the secondary cooling zone in continuous casting. *ISIJ International*. 1998;38(5):447-453. <http://dx.doi.org/10.2355/isijinternational.38.447>.
- 11 Mahapatra R, Brimacombe JK, Samarasekera IV, Walker N, Paterson E, Young J. Mold behavior and its influence on quality in the continuous casting of steel slabs: part I. Industrial trials, mold temperature measurements, and mathematical modeling. *Metallurgical Transactions*. 1991;22(6):861-874. <http://dx.doi.org/10.1007/BF02651163>.

- 12 Kumar S, Meech J, Samarasekera IV, Brimacombe JK, Rakocevik V. Development of intelligent mould for online detection of defects in steel billets. *Ironmaking & Steelmaking*. 1999;26(4):269-284. <http://dx.doi.org/10.1179/030192399677130>.
- 13 Paul A, Pradhan N, Ray A, Bhor P, Mazumdar S, Korath JM. Assessment of heat extraction through slab caster mould. *Scandinavian Journal of Metallurgy*. 2000;29(4):139-145. <http://dx.doi.org/10.1034/j.1600-0692.2000.d01-16.x>.
- 14 Guo L, Wang S, Zhan H, Yao M, Fang D. Mould Heat Transfer in the Continuous Casting of Round Billet. *ISIJ International*. 2007;47(8):1108-1116. <http://dx.doi.org/10.2355/isijinternational.47.1108>.
- 15 Gilles H. Primary and secondary cooling control. In: Cramb A. *The Making, Shaping and Treating of Steel*. 11th ed. Pittsburgh: AISE Steel Foundation; 2003. vol. 18.
- 16 Summerfield S, Fraser D. A new heat transfer correlation for impinging zone heat transfer on a hot steel plate. *Canadian Metallurgical Quarterly*. 2006;45(1):69-78. <http://dx.doi.org/10.1179/cmqr.2006.45.1.69>.
- 17 Samarasekera IV, Chow C. Continuous casting of steel billets. In: Cramb A. *The Making, Shaping and Treating of Steel*. 11th ed. Pittsburgh: AISE Steel Foundation; 2003. vol. 17.
- 18 Tutarova VD, Safonov D, Shapovalov N. Density distribution of the spray from flat spray nozzles in the secondary cooling zone of a continuous caster. *Metallurgist*. 2012;56(5-6):438-442. <http://dx.doi.org/10.1007/s11015-012-9594-8>.
- 19 Brimacombe J, Samarasekera IV, Lait J. Spray cooling in the continuous casting of steel. In: Brimacombe JK, Samarasekera IV, Lait JE. *Continuous Casting: Heat Flow, Solidification and Crack Formation*. Chelsea: Warrendale Iron and Steel Society; 1984. p. 109-123.
- 20 Zheng K, Petrus B, Thomas BG, Bentsman J. Design and implementation of a real-time spray cooling system for a continuous casting of thin steel slabs. In: Association for Iron & Steel Technology. *Proceedings of AISTech Steelmaking Conference*; 2007 May 7-10; Indianapolis, USA. Warrendale: AIST; 2007. p. 1-15.
- 21 Meng Y, Thomas BG. Heat transfer and solidification model of continuous slab casting: CONID. *Metallurgical and Materials Transactions. B, Process Metallurgy and Materials Processing Science*. 2003;34(5):685-705. <http://dx.doi.org/10.1007/s11663-003-0040-y>.
- 22 Wang H, Li G, Lei Y, Zhao Y, Dai Q, Wang J. Mathematical heat transfer model research for the improvement of continuous casting temperature. *ISIJ International*. 2005;45(9):1291-1296. <http://dx.doi.org/10.2355/isijinternational.45.1291>.
- 23 Patankar SV. *Numerical heat transfer and fluid flow*. United States: Taylor & Francis; 1980.
- 24 Flemings M. *Solidification processing*. New York: McGraw Hill; 1974.
- 25 Huang X, Thomas BG, Najjar B. Modeling of steel grade transition in continuous slab casting processes. *Metallurgical Transactions. B, Process Metallurgy*. 1992;23B:379-393.
- 26 Howe A. Estimation of liquidus temperature for steels. *Ironmaking & Steelmaking*. 1988;15:134-142.
- 27 Brimacombe J, Weinberg F, Hawbolt EB. Metallurgical investigation of continuous casting billet moulds. In: Brimacombe JK, Samarasekera IV, Lait JE. *Continuous Casting: Heat Flow, Solidification and Crack Formation*. Chelsea: Warrendale Iron and Steel Society; 1984. p. 73-84.
- 28 Ingerslev P, Henein H. An integral boundary approach for 1- and 2-D modeling of ingot reheating and cooling. *Ironmaking & Steelmaking*. 1997;24:75-85.
- 29 Hibbins S. *Characterization of heat transfer in the secondary cooling of a continuous slab* [master dissertation]. Vancouver: University of British Columbia; 1982.
- 30 El-Bealy M. Monotonic and fluctuated cooling approaches in secondary cooling zones during continuous casting. *Canadian Metallurgical Quarterly*. 1997;36(1):49-56. <http://dx.doi.org/10.1179/cmqr.1997.36.1.49>.
- 31 Cho K, Kim B. Numerical analysis of secondary cooling in continuous slab casting. *Journal of Materials Science and Technology*. 2008;24:389-390.

Received: 4 Jul. 2014

Accepted: 11 Aug. 2014